https://doi.org/10.48048/tis.2024.7924

Ethylene Adsorption on Alkali-Hydrophobic Zeolite Y

Nopbhasinthu Patdhanagul*, Piyanooch Nedkun and Keerati Maneesai

General Science Department, Faculty of Science and Engineering, Kasetsart University Chalermphrakiet Sakon Nakhon Province Campus, Sakon Nakhon 47000, Thailand

(*Corresponding author's e-mail: nopbhasinthu.p@ku.th)

Received: 3 January 2024, Revised: 6 March 2024, Accepted: 13 March 2024, Published: 10 June 2024

Abstract

Zeolites HY with different hydrophobicity having Si/Al ratios of 10, 100 and 750 were modified by an ion exchange process with nitrate solutions of alkali cations in the concentration range 0.1 - 100 mM. The modified samples were characterized by ICP-OES, XRD and surface analysis with N_2-adsorption. The ethylene adsorptivities of these modified zeolites were measured under degassed and non-degassed conditions. All zeolites showed the enhancement in ethylene adsorptivity upon modification, while the K^+ ions modified ones showed the best enhancement. The modified hydrophobic zeolites with Si/Al ratios of 100 and 750 showed no differences in adsorptivity under the degassed and non-degassed conditions. However, for less hydrophobic zeolite (Si/Al = 10), the adsorption under the degassed condition was much higher than the adsorption under the non-degassed condition. These results indicate that the modified hydrophobic zeolites with Si/Al ratios of 100 and 750 are suitable as ethylene scavengers at ambient conditions.

Keywords: Zeolite HY, Alkali metal cation modified zeolite, Ethylene adsorption, Hydrophobic zeolite

Introduction

Ethylene or ethene (C_2H_4) is a basic chemical building block in industrial synthesis of various chemical compounds such as polyethylene, styrene, polythene, synthetic rubbers, fuel components and other valuable chemicals [1-4]. High purity ethylene is often needed as a starting material, and it is typically obtained from steam cracking of naphtha or hydrocarbons. Ethane (C_2H_6) is usually produced as a by-product [5]. Separation of ethylene and ethane is not an easy process due to their similar molecular properties. They have very close boiling points, leading to similar volatility, and an enormous number of plates are needed for distillation towers to achieve a high degree of separation [6-9]. An alternative separation technique is cryogenic distillation which requires a high pressure and is also an energy-intensive separation method [10-13]. Currently, high-pressure distillation is used as the standard purification method due to its effectiveness and reliability. The rising demand for ethylene and the requirement for less energy consumption led to searches for alternative and more sustainable separation processes [14,15]. Removal of ethylene is also important in postharvest technology because ethylene is produced as a plant hormone during the growth process. Even in trace amounts, it can accelerate the ripening and aging of fruits, vegetables and floral products. This disruption results in morphogenetic and physiological changes leading to a downward curling of leaves and shoots, the abscission of flower buds, petals or leaves, water soaking of older leaves, wilting of flowers and speeding up of the ripening process. These actions of ethylene are not desirable during transportation and long-term storage. Removal of ethylene is needed to retard spoilage and reduce losses. Some of the techniques that are suitable for ethylene removal at either large or small scales are absorption, adsorption and membrane separation. Separation by gas adsorption has received active investigation due to its simplicity and low cost [16,17]. Several inorganic materials, such as activated carbon, activated alumina, silica gel and zeolite display excellent adsorptive property. Some of these materials show the ability to adsorb ethylene when metal cations are incorporated in their structures [18-27]. This selective adsorption property is the result of strong interaction between the unsaturated bond in the ethylene and the metal cations in the surface of adsorbent and this interaction is called π-complexation [28-37]. In order to produce a good adsorptive material, cations can be dispersed over a high porosity support. Zeolite is often employed due to its high surface area and porosity [38-44]. Zeolite contains some cations located inside its frameworks which allow effective exchanges with suitable cations.

Our previous studies [45,46] have reported the enhancement of ethylene adsorption of NaY zeolites that were modified with either alkali metal cations or cationic surfactants. In another study [47] we found that the ethylene adsorption ability was further enhanced upon combined modification with both alkali

metal cation (K^+) and a cationic surfactant (PTAB). Intensive analysis indicated that the alkali metal cations stayed mainly within the micropores of the zeolite to balance charges, while cationic surfactant with a long chain could not penetrate the internal surfaces and was only dispersed on the external surfaces to provide more adsorption sites for ethylene molecules.

Due to the hydrophilic property to zeolite NaY (Si/Al ratio = 2), the ethylene adsorbent that we had developed showed competitive water adsorption. At ambient conditions, water molecules filled up the adsorption sites and ethylene adsorptivity only showed up after degassing. This ethylene adsorbent is, therefore, suitable for use in an ethane-ethylene separation plant since the working condition involves high temperature which limits traces of water.

Development of an ethylene adsorbent that works well in ambient conditions, hydrophobic zeolite may be a suitable candidate. Zeolites tend to be more hydrophobic with an increase in the SiO_2/Al_2O_3 ratio. However, these hydrophobic zeolites lose the ethylene adsorption capacity as the cation number within the framework decreases with increase of the Si:Al ratio. Modification of hydrophobic zeolite by suitable cations would increase the capacity for ethylene adsorption while water adsorption is eliminated.

The objective of this paper is to investigate the ethylene adsorption capacity on hydrophobic Y zeolites with different Si:Al ratios. The hydrophobic zeolites are modified with group I metal cations to search for the cation that enhances ethylene adsorption to the greatest extent. For homogeneity, commercially available zeolite Y with Si:Al ratios of 10, 100 and 750 are used as supports and nitrate solutions of Li^+, Na^+, K^+, Rb^+ and Cs^+ ions in the concentration range of 0.1 - 100 mM are used to modify these zeolites. Ethylene adsorption is studied under degassed and non-degassed conditions.

Materials and methods

Modification of zeolite Y by alkali metal cations

Zeolites HY with 3 different Si/Al ratios of 10, 100 and 750 (Tosoh, Japan) were exchanged with nitrate solutions of Li^+, Na^+, K^+, Rb^+ and Cs^+ in the concentration range 0.1 - 100 mM. Nitrate salts of alkali metal cations were purchased from Sigma Aldrich, Germany (Na^+, K^+) and Fluka, Japan (Li^+, Rb^+ and Cs^+). The suspension was stirred at ambient condition for 24 h (solid/liquid ratio = 2.0 g L^{-1}), then the solid and liquid fractions were separated by filtration. The solid phases were washed 3 times with deionized water and dried at 383.15 K for 3 h. Twelve modified samples together with 3 original purchased samples were characterized for crystallinity by x-ray diffraction, for surface properties by N_2 adsorption and were studied for ethylene adsorptivity under degassed and non-degassed conditions. For simplicity, the samples will be referred to by their modified cation and Si/Al ratio. For example, HY10, HY100 and HY750 are zeolite hydrogen Y with Si/Al ratios of 10, 100 and 750, respectively. Li-HY10 is an abbreviation for zeolite HY with a Si/Al ratio of 10 that was modified with Li^+ ion. Therefore, the 15 samples under investigation were, HY10, HY100, HY750, Li-HY10, Li-HY100, Li-HY750, Na-HY10, Na-HY100, Na-HY750, K-HY10, K-HY100, K-HY750, Rb-HY10, Rb-HY100, Rb-HY750, Cs-HY10, Cs-HY100 and Cs-HY750. Additionally, the concentration of salt solution will be added in front of these abbreviations.

Characterization

The zeolite samples were evaluated for crystallinity by powder X-ray diffraction (XRD) using XRD Bruker D8 advance with Cu Kα radiation at room temperature. The scanning speed was 0.5 ° per second in the 2 θ range 5 - 60 ° with 0.02 ° as the step size. The crystalline size and crystallinity percentage were collected from Eqs. (1) and (2), respectively.

$$D_{hkl} = \frac{0.9\lambda}{\beta \cos\theta} \quad (1)$$

$$\text{crystallinity percentage}(\%) = \frac{\text{total area of twelve strong peak of modified zeolite}}{\text{total area of twelve strong peak of unmodified zeolite Y}} \times 100 \quad (2)$$

The former equation is Scherrer's equation, where D_{hkl} is the crystalline size, λ is the wavelength of the radiation that equals 0.154056 nm for Cu Kα, β is the line broadening of the peak taken from full width at half maximum (FWHM) and θ is the angle of the diffraction peak. The latter equation is applied to calculate the crystallinity percentage. This percentage is obtained from the peak area ratio of modified and unmodified zeolite Y.

Particle characterization of these adsorbents, such as the Brunauer-Emmett-Teller (BET) surface area, external surface area, micropore surface area, total pore volume, micropore volume, pore size distribution and average pore diameter were obtained by a volumetric method of N_2 adsorption at 77.15 K using BELSORPMAX (Microtrac MRB, Japan). The BET surface area is the sum of external and internal surface areas. Internal or micropore surface area can be obtained from the adsorption isotherm by the t-plot method [48,49]. The elemental analyses of alkali were carried out by the inductively coupled plasma optical emission spectroscopic technique (ICP-OES, Perkin Elmer).

Ethylene adsorption

The ethylene gas adsorption ability of the modified materials was investigated using BELSORPMAX (Microtrac MRB, Japan). Ethylene gas with 99.999 % purity was obtained from MOX (Malaysia). The adsorbents were studied under 2 conditions: 1) The degassed condition in which the sample was degassed at 573.15 K for 3 h before measurement and 2) The non-degassed condition in which the samples were studied for ethylene adsorption without degassing. The ethylene adsorption studies were performed at adsorptive temperature of 273.15 K in the pressure range from 0 to 1 atm. Each sample was performed in 5 measurements and each isotherm displayed in this manuscript was an average of 5 reproducible measurements.

Results and discussion

Characterization

The x-ray diffraction patterns of zeolite HY before and after modification are displayed in **Figures 1(a) - 1(c)**. All diffractograms display the single phase for which the major diffraction planes are (1 1 1), (2 2 0), (3 1 1), (3 3 1), (5 1 1), (4 4 0), (5 3 3), (6 4 2), (7 3 3), (5 5 5), (8 4 0) and (6 5 5). These diffraction planes occurred at the 2 θ angle of 6.2, 10.2, 12.0, 15.8, 19.2, 20.5, 23.9, 27.0, 29.4, 31.5, 32.3 and 37.5 °. The areas of these 12 major peaks were used to calculate the percentage crystallinity. The values for crystalline size and crystallinity percentage are also presented in the figure. From the values of percentage crystallinity displayed in **Figure 1**, it is clearly seen that ion exchange of H^+ with small group I cations Li^+ and Na^+ led to only slight destruction of the crystal structure (< 10 %). However, for exchanges with larger cations K^+, Rb^+ and Cs^+, crystal destruction is quite pronounced (up to ~ 25 % for Cs^+ exchanges). The destruction order increases as $Li^+ < Na^+ < K^+ < Rb^+ < Cs^+$. When the crystal destructions were compared among 3 zeolites with different hydrophobicity, it seemed that the zeolite with Si/Al ratio of 100 could maintain the crystallinity slightly better than the other 2. For example, percentage crystallinities of Li-HY10, Li-HY100 and Li-HY750 were 97.7, 98.5 and 96.6 %, respectively. Although small, this effect was systematic for all exchanged cations.

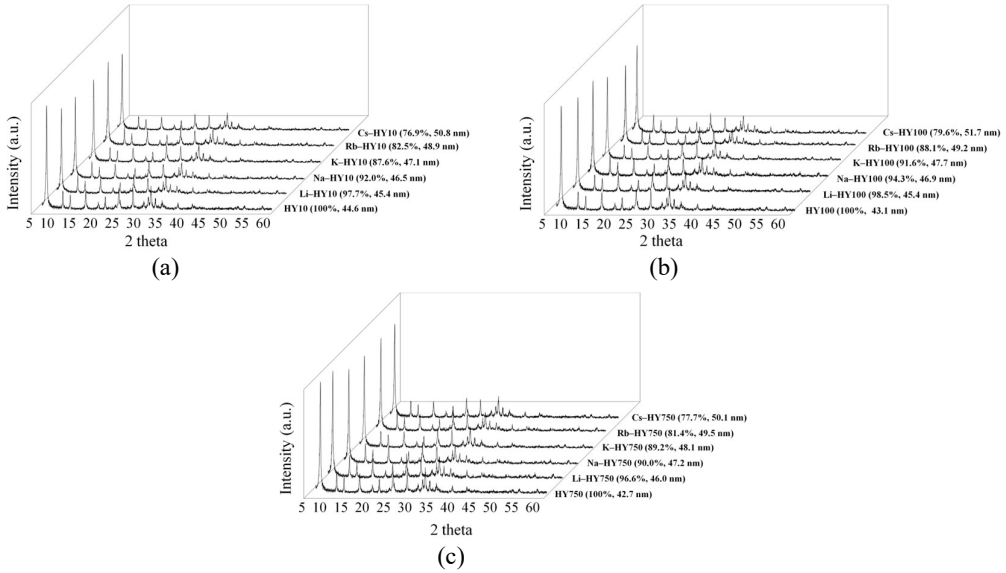

Figure 1 The x-ray diffraction pattern of zeolite HY modified with 5.0 mM alkali cations. (a) HY10, (b) HY100 and (c) HY750. The percentage crystalinity and particle size are presented in parentheses.

When particle sizes (D_{hkl}) were considered, it appeared that the particle sizes of unmodified zeolites decreased in the order HY10 (44.6 nm) > HY100 (43.1 nm) > HY750 (42.7 nm). These differences may be because of de-alumination in which the large cation Al^{3+} (0.054 nm) was replaced by smaller cations Si^{4+} (0.040 nm), leading to slightly smaller crystallites. The particle sizes of modified zeolites increased with the increase in size of the exchanged cations. This effect, together with the lower percentage crystallinity for large ion exchanges, indicates that the insertion of larger cations into the zeolite pores slightly destroys pore structure and enlarges the particle sizes.

Considering the effect of solution concentration, the percentage crystallinity of HY100 zeolite modified with group I metal nitrate solutions of different concentrations are listed in **Table 1**. For very dilute solution (1.0 mM), the percentage crystallinities were as high as 98.9 % for Li-HY100, 95.9 % for K-HY100 and 85.8 % for Cs-HY100. For higher concentration (100 mM), the percentage crystallinities decreased to 83.3 % for Li-HY100 69.1 % for Cs-HY100. Similar results were observed for modified HY10 and HY750 (data are not presented). This information suggests that ethylene adsorption may be higher for zeolite modified at low cation concentration, since the crystallinities were well preserved.

Table 1 Percentage crystallinities of zeolite HY100 modified with group I metal cations at different concentrations.

Concentration (mM)	Percentage crystallinity (%)				
	Li-HY100	**Na-HY100**	**K-HY100**	**Rb-HY100**	**Cs-HY100**
0.5	99.4	98.6	98.1	96.7	95.1
1.0	98.9	96.4	95.9	92.3	85.8
5.0	98.5	94.3	91.6	88.1	79.6
10.0	97.2	91.9	89.7	83.4	75.2
25.0	94.0	87.6	86.4	77.8	74.8
50.0	91.6	83.8	82.5	74.1	72.5
75.0	88.8	81.1	80.8	73.5	70.8
100.0	83.3	79.9	79.6	70.9	69.1

The results from particle analyses contain details about surface area, pore volumes and pore diameters. For the brevity of this report, only selective data are presented. In **Table 2**, the surface areas of unmodified and modified zeolites are displayed and only the data of the maximum surface area achieved by the modification with each cation are given. Investigation of the surface area of the unmodified zeolite HY (HY10, HY100 and HY750) revealed that the total BET surface area increased with increase of hydrophobicity. Similar observations have been reported in other works [50,51]. However, with detailed investigation, while the external surface area increased with increases in hydrophobicity, the micropore surface area decreased in the opposite direction. Explanation of these phenomena, information from x-ray data is needed. X-ray diffraction results indicate that hydrophobic zeolite HY has smaller crystallite size due to replacement of large Al^{3+} ions by smaller Si^{4+} ions. Therefore, the resulting hydrophobic zeolite had less micropore area. Another effect of dealumination was destruction of crystallinity of the zeolite, leading to higher external surface area.

Table 2 External, micropore and BET surface area of unmodified HY zeolites and HY zeolites modified with group I metal cations. Only modifications that gave rise to highest surface area are presented in this table.

Adsorbent	Surface area (m^2 g^{-1})		
	External	**Micropore**	**BET**
HY10	76.9	672.7	749.6
HY100	107.7	649.4	757.1
HY750	154.3	614.5	768.8
25.0 mM Li-HY10	81.7	725.1	806.8
10.0 mM Na-HY10	81.3	725.2	806.5
10.0 mM K-HY10	82.5	732.3	814.8
10.0 mM Rb-HY10	81.5	711.7	793.2

Adsorbent	Surface area (m^2 g^{-1})		
	External	Micropore	BET
10.0 mM Cs-HY10	82.7	711.4	794.1
10.0 mM Li-HY100	113.9	696.6	810.5
5.0 mM Na-HY100	115.5	709.8	825.3
5.0 mM K-HY100	116.2	720.6	836.8
2.5 mM Rb-HY100	117.8	693.5	811.3
2.5 mM Cs-HY100	117.1	695.3	812.4
10.0 mM Li-HY750	181.4	687.0	868.9
5.0 mM Na-HY750	176.9	714.4	891.3
5.0 mM K-HY750	179.6	712.8	892.4
2.5 mM Rb-HY750	176.9	684.7	861.6
2.5 mM Cs-HY750	182.5	691.4	873.9

For modified zeolites, the results show a few interesting points: The modification led to increases of BET surface area which could be attributed to increases of micropore surface area. Changes of external surface area were rather small and independent of modified cations. For example, the external surface area of 25.0 mM Li-HY10 was 81.7 m^2 g^{-1} and was comparable to 82.7 m^2 g^{-1} for 10.0 mM Cs-HY10.

Due to destruction of crystallinity at high concentration modification, the BET surface area showed high values at low concentration modification. For large cations such as Cs^+ modification, high surface area was achieved upon modification with very dilute solution (2.5 mM).

Modification with K^+ ion gave rise to highest values of BET surface areas for all modified HY10, HY100 and HY750 and the modification concentrations were as low as 5 - 10 mM. The ability of cations in promoting the micropore and BET surface area ranks in the order $Li^+ < Na^+ < K^+$. Larger cations such as Rb^+ and Cs^+ did not produce higher values of surface area. This phenomenon may be the result of balances between interaction of the cations with N_2 probing gas, destruction effect and the cation population within the micropores.

Analyses of the metal contents within the zeolite frameworks were done by ICP optical emission spectroscopic technique and the mole% of the alkali metal cations are displayed in **Table 3**. For modification with very dilute alkali solution (1.0 mM), the content of all 5 metal cations were comparable for modified HY100 and HY750 (≈ 0.11 - 0.13 mole%). For modified HY10 which was less hydrophobic, the metal content was slightly higher (≈ 0.13 - 0.15 mole%). For modification at higher concentration (10.0 mM), the metal contents for Li^+, Na^+ and K^+ were comparable in the range 1.16 - 1.35 mole% for HY100 and HY750 and the values for HY10 were slightly higher at 1.35 - 1.40 mole%. However, for Rb^+ and Cs^+ modification, the metal contents dropped to 1.06 - 1.22 for all zeolites. This result indicates that the ability for larger cations to enter into the zeolite framework was less than that of the smaller ions. Similar results were observed for modification at higher concentration (100 mM).

Table 3 The content in mole% of group I metal cations within the zeolite framework at different concentration.

Cation concentration (mM)		Mole% of alkali cations in modified zeolite HY				
		Li^+	Na^+	K^+	Rb^+	Cs^+
1.00	HY10	0.14	0.15	0.14	0.13	0.13
	HY100	0.12	0.13	0.13	0.12	0.11
	HY750	0.11	0.11	0.11	0.11	0.11
10.0	HY10	1.35	1.35	1.40	1.22	1.18
	HY100	1.16	1.24	1.22	1.06	1.10
	HY750	1.16	1.35	1.31	1.10	1.07
100	HY10	9.90	10.26	9.82	6.06	5.50
	HY100	8.95	9.56	9.92	5.37	5.40
	HY750	9.98	9.07	9.13	5.39	5.34

The interaction between group I cations within the zeolite framework and the N_2 probing gas is dominated by interaction of the quadrupole moment of N_2 with the electrostatic fields in the zeolite. The small cations (not large cations) improve N_2 capacity because they have a higher charge density, produce stronger electrostatic fields in the zeolite and adsorb N_2 more strongly. So, the smaller ions gave rise to higher surface area together with the destruction of the zeolite framework by larger cations, led to a decreased surface area. K^+ modified zeolites appeared to have the highest surface area.

There is no significant difference in the values for pore volume of all zeolites. The total pore volumes were in the range of 0.42 - 0.48 $cm^3\ g^{-1}$ and the micropore volumes were in the range of 0.30 - 0.34 $cm^3\ g^{-1}$. The pore volumes of the unmodified zeolites were slightly less than those of the modified ones.

Ethylene adsorption isotherm

Two types of interactions could occur upon the adsorption of ethylene onto zeolite surface (**Figure 2**). The cation-π interaction as already described is responsible for interaction between the π-orbital of ethylene and the empty metal s or d orbital. This interaction favors the larger size of cation. Another significant interaction is called CH-O interaction. The weak hydrogen bond as CH-O interaction is the bonding between an electronegative oxygen atom at the zeolite surface and weakly electropositive hydrogen atoms on the ethylene molecules [52-54]. The blockage and reduction of the available oxygen adsorption sites nearby would present according to the presence of larger cation within the framework. These 2 opposite effect interactions control the ethylene adsorptivity of the zeolite framework.

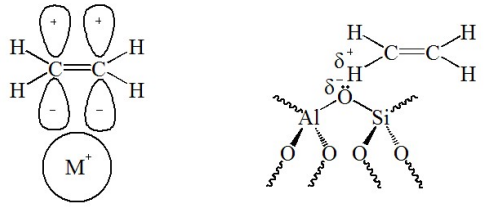

(a) (b)

Figure 2 Possible interactions between ethylene and the modified zeolite HY: (a) Cation-π and (b) CH-O.

The ethylene adsorption isotherm of all samples displayed a typical adsorption isotherm of type I as described by IUPAC. The ethylene adsorption capacities of all samples increased rapidly in the low relative pressure region and became linear in the high relative pressure region. The ethylene adsorption experiments were performed under degassed and non-degassed conditions and the maximum adsorption at relative pressure of 1 are displayed in **Table 4**.

Table 4 Maximum ethylene adsorbed volume at relative pressure $P/P_o \approx 1$ of non-modified (H^+) and modified zeolites with the Si/Al ratio of 10, 100 and 750.

Cation	Maximum ethylene adsorbed volume ($cm^3\ g^{-1}$)					
	HY10		HY100		HY750	
	degassed	non-degassed	degassed	non-degassed	degassed	non-degassed
unmodified	64.91	57.20	48.68	43.41	42.60	39.50
Li^+	73.55	8.65	55.16	55.16	49.03	47.81
Na^+	79.20	9.98	60.26	59.40	50.91	50.91
K^+	81.36	10.63	61.52	61.02	54.24	53.33
Rb^+	67.82	6.56	50.57	51.00	44.62	44.62
Cs^+	69.61	6.71	52.06	51.94	47.89	47.81

Table 4 compares the ethylene adsorptivity of the 3 zeolites under degassed and non-degassed conditions. Under both conditions, these 3 unmodified zeolites showed high ability to adsorb ethylene although the adsorptivity under degassed condition was slightly higher than that of non-degassed. This result indicates the presence of a small amount of water molecule adsorption within all the zeolite frameworks. The order of the ethylene adsorptivity decreased as HY10 > HY100 > HY750. This

phenomenon results from the lowering of the Al^{3+} ions along the series which leads to lesser charge balancing proton to interact with ethylene through the cation-π interaction.

Upon modification with alkali metal cations, HY100 and HY750 showed higher ethylene adsorptivity and the extents of adsorption are almost equal for both degassed and non-degassed samples. However, the modified HY10 lost its ability to adsorb ethylene under the non-degassed condition while the degassed samples showed very high ethylene adsorption. The ethylene adsorption dropped from 57.20 cm^3 g^{-1} for unmodified HY10 to as low as 6.71 cm^3 g^{-1} for Cs^+-modified HY10. The contrast is in ethylene adsorptivity of the modified HY10 under the degassed and non-degassed conditions is displayed in **Figure 3**. The sodium cations have greater water adsorption sites than protons do as the resulted in water adsorption of hydrophobic of Na-ZSM-5 and H-ZSM-5 [55]. HY10 with rather high Si/Al ratio possesses quite high number of Al^{3+} ions and the replacement of the charge balanced protons with group I metal cations gave rise to higher water adsorption sites. Therefore, the substrate became hydrophilic. It appears that the water adsorption and the ethylene adsorption at the cationic site within the zeolite framework are competitive. In the case of HY10 which is rather hydrophilic, water adsorption is predominated and the modified HY10 cannot adsorb ethylene prior to degassing. However, For HY100 and HY750 the hydrophobic nature of the surface favors ethylene adsorption and the modified samples can adsorb the same amount of ethylene under both the degassed and non-degassed conditions.

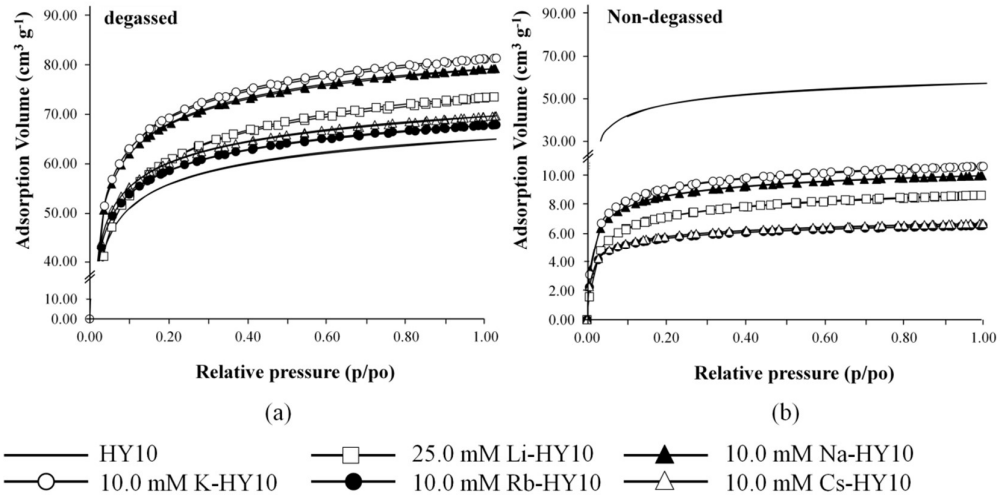

Figure 3 Ethylene adsorption isotherms of HY10 modified with group I metal cations under degassed (a) and non-degassed (b) conditions.

Now we turn our interest on the selection of the best cation for the modification. For adsorption under the degassed condition (**Table 4**), the ethylene adsorption values increased in order with modification with Li^+ and Na^+ ions and reached the highest value with K^+ modification. Enhancement of the adsorption by Rb^+ and Cs^+ modifications were also observed, but the extent of the adsorption was lower than that of K^+-modified zeolites. These phenomena correlated well with the results from the surface analysis which also indicated that K^+-modified zeolite possesses the highest surface area. Ethylene adsorption on the zeolite surface is controlled by 2 interactions that have opposite effects. The cation-π favors large cations but the large cations block the oxygen sites of the CH-O interaction. The balance of these 2 interactions together with a lesser amount of larger cation within zeolite pores results in K^+-modified zeolite being the best adsorbent for ethylene. For adsorption under the non-degassed condition, hydrophobic zeolite HY100 and HY750 showed results like the results of the degassed condition. The best ethylene adsorption capacity at ambient condition (non-degassed) was found to be 61.02 cm^3 g^{-1} when HY100 was modified with 5.0 mM K^+ solution. For K^+ modification of HY10 which is less hydrophobic, ethylene adsorption at ambient (non-degassed) condition was low (10.63 cm^3 g^{-1}) but the adsorption under the degassed condition showed the highest adsorptivity of 81.36 cm^3 g^{-1}.

An important aspect to point out from **Table 4** is that the modified hydrophobic zeolites (HY100 and HY750) displayed similar ethylene adsorptivity for both degassed and non-degassed conditions. These modified zeolites are, therefore, effective for ethylene removal at ambient conditions. The less hydrophobic zeolite (HY10) could less adsorb ethylene at ambient conditions. However, upon removal of guest

molecules within the pores (degassed), its ethylene adsorptivity increased and it could adsorb ethylene better than the other 2 more hydrophobic zeolites.

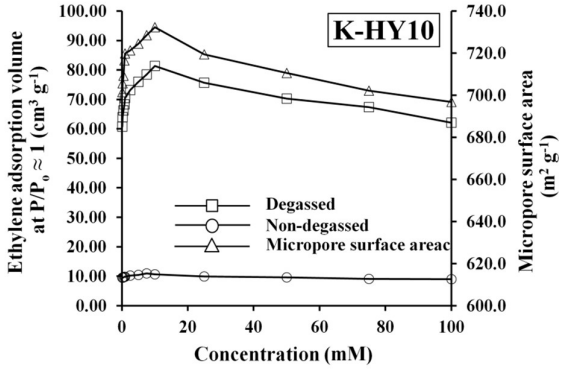

(a)

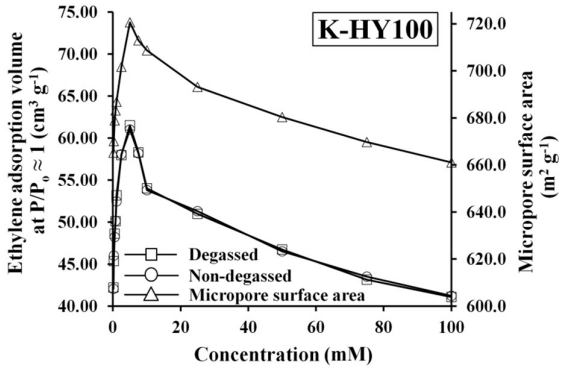

(b)

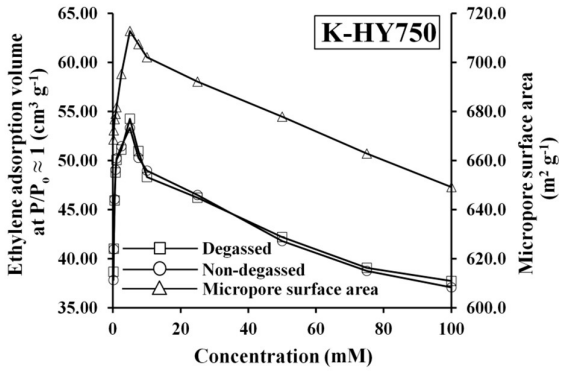

(c)

Figure 4 The correlation between micropore surface area (△) and maximum ethylene adsorption volume at $P/P_o \approx 1$ under degassed (□) and non-degassed (○) conditions of (a) K-HY10 (b) K-HY100 and (c) K-HY750.

Very strong correlations between micropore surface area and maximum ethylene adsorption volume at P/Po ≈ 1 are displayed in **Figure 4** for K^+ modified zeolites. Similar plots for a correlation with the BET surface area were also investigated, but no correlation could be observed. This indicates that ethylene adsorption occurred within the micropores of zeolite, and thus, K^+-modified zeolite, which possesses the highest micropore area, is the best support for effective ethylene adsorption.

The comparison of ethylene adsorption efficiency on to zeolite materials between this work and our previous works is summarized in **Table 5**. It is clearly seen that hydrophobic zeolite presented the great value of ethylene adsorption volume, but the preheated step is required. While hydrophobic zeolites have a great potential for ethylene adsorption is no need for a preheated process.

Table 5 The comparison of ethylene adsorption efficiency on to zeolite materials.

Materials	Ethylene adsorption volume ($cm^3\ g^{-1}$)	Preheated temperature (K)	Temperature (K)	Reference
K+-zeolite HY10	81.36	523.15	273.15	This work
K+-zeolite HY10	10.63	No preheating	273.15	This work
K+-zeolite HY100	61.52	523.15	273.15	This work
K+-zeolite HY100	61.02	No preheating	273.15	This work
K+-zeolite HY750	54.23	523.15	273.15	This work
K+-zeolite HY750	53.33	No preheating	273.15	This work
K+-zeolite NaY	102.45	523.15	273.15	[45]
Rb+-zeolite NaY	98.50	523.15	273.15	[45]
Cs+-zeolite NaY	90.15	523.15	273.15	[45]
PTAB-zeolite NaY	104.60	523.15	273.15	[46]
OTAB-zeolite NaY	95.82	523.15	273.15	[46]
HTAB-zeolite NaY	74.38	523.15	273.15	[46]
DDAB-zeolite NaY	64.51	523.15	273.15	[46]
K+/PTAB-zeolite NaY	110.10	523.15	273.15	[47]
PTAB/K+-zeolite NaY	109.40	523.15	273.15	[47]
PTAB + K+/zeolite NaY	116.60	523.15	273.15	[47]

Conclusions

Three HY-zeolites with different degrees of hydrophobicity were modified by alkali cations. The XRD indicated the modification of zeolites with the exchange solutions did not lead to significant structural changes especially at low concentration exchanges. Ion exchanges with large cations showed some destruction of crystallinity and the particle sizes increased with the increase in size of the exchange cations. The BET surface area increased with increases in hydrophobicity while the micropore area decreased in the opposite direction. Modification with alkali cations increased the micropore surface area, zeolite HY10 modified with 10.0 mM K^+ ions showed the highest micropore surface area. For more hydrophobic zeolite, HY100 displayed slightly less micropore area when modified with 5.0 mM K^+ ions. The K^+ ion seemed to be the best ion to promote an increase of micropore surface area because of balances between destruction effects, cation population within the micropores, and the strength of interaction between cations and N_2-probing gas. For the ethylene adsorption study, the correlation between ethylene adsorptivity and the micropore surface area indicated that adsorption occurs within the micropore of the zeolite framework. HY100 zeolite modified with 5.0 mM K^+ solution showed the ability to adsorb the highest volume of ethylene at ambient conditions and it is suitable to be used as an ethylene scavenger in the post harvesting process. For modified HY10, the ethylene adsorption was low upon adsorption at ambient conditions, but the ethylene adsorption increased drastically upon degassing with the highest ethylene adsorption volume (81.36 $cm^3\ g^{-1}$) of 10.0 mM K^+ modified HY10. This compound may be useful in a large-scale industrial ethylene-ethane separation process.

Acknowledgements

The authors would like to thank Faculty of Science and Engineering, Kasetsart University Chalermphrakiet Sakon Nakhon Province Campus, Thailand, for research equipment and financial support.

References

[1] W Gerhartz. *Ullman's encyclopedia of industrial chemistry*. 5th eds. Wiley-VCH Verlag GmbH & Co. KGaA, Weinheim, Germany, 1987, p. 45-93.

[2] HT Wang, DM Lin and XP Zhou. Ethylene synthesis from the oxidative bromination of ethane. *Appl. Catal. A Gen.* 2009; **364**, 130-6.

[3] S Matar and LF Hatch. *Chemistry of petrochemical processes*. 2nd eds. Gulf Professional Publishing, Texas, 2001.

[4] T Ren, M Patel and K Blok. Olefins from conventional and heavy feedstocks: Energy use in steam cracking and alternative processes. *Energy* 2006; **31**, 425-51.

[5] JA Moulijn, M Makkee and AEV Diepen. *Chemical process technology.* 2nd eds. John Wiley & Sons, Chichester, 2013.

[6] KM Sundaram, MM Shreehan and EF Olszewski. *Ethylene*. *In*: JI Kroschwitz and GM Howe (Eds.). Kirk-Othmer encyclopedia of chemical technology. 4th eds. John Wiley & Sons, New York, 1994, p. 877-915.

[7] AV Miltenburg, W Zhu, F Kapteijn and JA Moulijn. Adsorptive separation of light olefin/paraffin mixtures. *Chem. Eng. Res. Des.* 2006; **84**, 350-4.

[8] M Bordonhos, M Lourenço, JRB Gomes, P Ferreira and ML Pinto. Exploring periodic mesoporous organosilicas for ethane-ethylene adsorption-separation. *Microporous Mesoporous Mater.* 2021; **317**, 110975.

[9] J Pires, J Fernandes, AC Fernandes and M Pinto. Reverse selectivity of zeolites and metal-organic frameworks in the ethane/ethylene separation by adsorption. *Separ. Sci. Tech.* 2017; **52**, 51-7.

[10] GE Keller, AE Marcinkowsky, SK Verma and KD Williamson. *Olefin recovery, and purification via silver complexation. In*: NN Li and JM Calo (Eds.). Separation and purification technology, Maecel Dekker, New York, 1992, p. 59-83.

[11] Y Wang, SB Peh and D Zhao. Alternatives to cryogenic distillation: Advanced porous materials in adsorptive light olefin/paraffin separations. *Small* 2019; **15**, 1900058.

[12] J Pires, J Fernandes, K Dedecker, JRB Gomes, G Pérez-Sánchez, F Nouar, C Serre and ML Pinto. Enhancement of ethane selectivity in ethane-ethylene mixtures by perfluoro groups in Zr-based metal-organic frameworks. *ACS Appl. Mater. Interfaces* 2019; **11**, 27410-21.

[13] H Abdi, H Maghsoudi and V Akhoundi. Adsorption properties of ion-exchanged SSZ-13 zeolite for ethylene/ethane separation. *Fluid Phase Equil.* 2021; **546**, 113171.

[14] RB Eldridge. Olefin/paraffin separation technology: A review. *Ind. Eng. Chem. Res.* 1993; **32**, 2208.

[15] DJ Safarik and RB Eldridge. Olefin/paraffin separation by reactive adsorption: A review. *Ind. Eng. Chem. Res.* 1998; **37**, 2571-81.

[16] Y Liu, M Tang, M Liu, D Su, J Chen, Y Gao, M Bouzayen and Z Li. The molecular regulation of ethylene in fruit ripening. *Small Methods* 2020; **4**, 1900485.

[17] H Wei, F Seidi, T Zhang, Y Jin and H Xiao. Ethylene scavengers for the preservation of fruits and vegetables: A review. *Food Chem*. 2021; **33**, 127750.

[18] ZE Lim, QB Thai, DK Le, TP Luu, PTT Nguyen, NHN Do, PK Le, N Phan-Thien, XY Goh and HM Duong. Functionalized pineapple aerogels for ethylene gas adsorption and nickel (II) ion removal applications. *J. Envion. Chem. Eng*. 2020; **8**, 104524.

[19] B Erdoğan, M Sakızcı and E Yörükoğulları. Characterization and ethylene adsorption of natural and modified clinoptilolites. *Appl. Surf. Sci.* 2008; **254**, 2450-7.

[20] H Li, L Shi, C Li, X Fu, Q Huang and B Zhang. Metal-organic framework based on α-cyclodextrin gives high ethylene gas adsorption capacity and storage stability. *ACS Appl. Mater. Interfaces* 2020; **12**, 34095-104.

[21] AJ Rieth, AM Wright and M Dinca. Kinetic stability of metal-organic frameworks for corrosive and coordinating gas capture. *Nat. Rev. Mater.* 2009; **4**, 708-25.

[22] M Hazel Álvarez-Hernández, F Artés-Hernández, F Ávalos-Belmontes, MA Castillo-Campohermoso, JC Contreras-Esquivel, JM Ventura-Sobrevilla and GB Martínez-Hernández. Current scenario of adsorbent materials used in ethylene scavenging systems to extend fruit and vegetable postharvest life. *Food Bioprocess Tech.* 2008; **11**, 511-25.

[23] RW Triebe, FH Tezel and KC Khulbe. Adsorption of methane, ethane and ethylene on molecular sieve zeolite. *Gas Separ. Purif.* 1996; **10**, 81-4.

[24] AV Miltenburg, W Zhu, F Kapteijn and JA Moulijn. Adsorptive separation of light olefin/paraffin mixture. *Chem. Eng. Res. Des.* 2006; **84**, 350-4.

[25] A Anson, CCH Lin, TM Kuznicki and SM Kuznicki. Separation of ethylene/ethane mixture by adsorption on small-pored titanosilicate molecular sieves. *Chem. Eng. Sci.* 2010; **65**, 807-11.
[26] PO Graf and L Lefferts. Reactive separation of ethylene from the effluent gas of methane oxidative coupling via alkylation of benzene to ethylbenzene on ZSM-5. *Chem. Eng. Sci.* 2009; **64**, 2773-80.
[27] A Anson, Y Wang, CCH Lin, TM Kuznicki and SM Kuznicki. Adsorption of ethane and ethylene on modified EST-10. *Chem. Eng. Sci.* 2008; **63**, 4171-5.
[28] M Herberhold. *Metal π-complexes: Part II: Specific aspect.* Elsevier, Amsterdam, Netherlands, 1974.
[29] FJ Blas, LF Vega and KE Gubbins. Modeling new adsorbent for ethylene/ethane separation by adsorption via π-complexation. *Fluid Phase Equil.* 1998; **150**, 117-24.
[30] SU Rege, J Padin and RT Yang. Olefin/paraffin separations by adsorption: π-complexation vs. kinetic separation. *AIChE J.* 1998; **44**, 799-809.
[31] J Shen, JM Hill, RM Watwe, BE Spiewak and JA Dumesic. Microcalorimetric, infrared spectroscopic and DFT studied on ethylene adsorption on Pt/SiO_2 and $Pt-Sn/SiO_2$ catalysts. *J. Phys. Chem. B* 1999; **103**, 3929-34.
[32] XL Cao, Y Liu, GL Li, ZX Lu, S Li, ZM Cao and YG Huang. A 3D supramolecular framework assembled via π···π interactions and CH···Cl hydrogen-bonds with second-harmonic generation response *J. Mol. Struct.* 2021; **1244**, 130958.
[33] MN Ahmed, H Andleeb, AM Fahim, M Madni, SW Khan, B Kaboudin, MAA Ibrahim, PA Sidhom and DM Gil. Supramolecular assembly involving weak hydrogen bonds, anti-parallel π···π stacking and O···C tetrel bonding interactions and LOX studies in a 1H-pyrazol-1-yl)thiazole-4-carboxylate derivative: An experimental and theoretical study. *J. Mol. Struct.* 2024; **1296**, 136908.
[34] T Steiner. The hydrogen bond in the solid state. *Angew. Chem.* 2002; **41**, 48-76.
[35] EA Meyer, RK Castellano and F Diederich. Interactions with aromatic rings in chemical and biological recognition. *Angew. Chem.* 2003; **42**, 1210-50.
[36] M Nishio. The CH/π hydrogen bond in chemistry. Conformation, supramolecules, optical resolution and interactions involving carbohydrates. *Phys. Chem. Chem. Phys.* 2021; **13**, 13873-900.
[37] DT Infield, A Rasouli, GD Galles, C Chipot, E Tajkhorshid and CA Ahern. Cation-π interactions and their functional roles in membrane proteins. *J. Mol. Biol.* 2021; **433**, 167035.
[38] DW Breck. *Zeolite Molecular sieves: Structure, chemistry, and use.* John Wiley & Sons, New Jersey, 1974.
[39] A Dyer. *An introduction to zeolite molecular sieves*. John Wiley & Sons, New Jersey, 1988.
[40] SM Auerbach, KA Carrado and PK Dutta. *Handbook of zeolite science and technology.* Marcel Dekker, New York, 2003.
[41] DN Stamires. Properties of zeolite, faujasite, substitutional series: A review with new data. *Clays Clay Miner.* 1973; **21**, 379-89.
[42] D Vargas-Hernandez, MA Perez-Cruz and R Hernandez-Huesca. Selective adsorption of ethylene over ethane on natural mordenite and on K+-exchanged mordenite. *Adsorption* 2015; **21**, 153-63.
[43] GP Barbosa, HS Debone, P Severino, EB Souto and CFD Silva. Design and characterization of chitosan/zeolite composite films - Effect of zeolite type and zeolite dose on the film properties. *Mater. Sci. Eng. C* 2016; **60**, 246-54.
[44] H Yang, C Ma, X Zhang, Y Li, J Cheng and Z Hao. Understanding the active sites of Ag/zeolites and deactivation mechanism of ethylene catalytic oxidation at room temperature. *ACS Catal.* 2018; **8**, 1248-58.
[45] N Sue-Aok, T Srithanratana, K Rangsriwatananon and S Hengrasmee. Study of ethylene adsorption on zeolite NaY modified with group I metal ions. *Appl. Surf. Sci.* 2010; **256**, 3997-4002.
[46] N Patdhanagul, T Srithanratana, K Rangsriwatananon and S Hengrasmee. Ethylene adsorption on cationic surfactant modified zeolite NaY. *Microporous Mesoporous Mater.* 2010; **131**, 97-102.
[47] N Patdhanagul, K Rangsriwatananon, K Siriwong and S Hengrasmee. Combined modification of zeolite NaY by phenyl trimethyl ammonium bromide and potassium for ethylene gas adsorption. *Microporous Mesoporous Mater.* 2012; **153**, 30-4.
[48] JHD Boer, BG Linsen and TJ Osinga. Studies on pore systems in catalysts: VI. The universal *t* curve. *J. Catal.* 1965; **4**, 643-8.
[49] JHD Boer, BC Lippens, BG Linsen, JCP Broekhoff, AVD Heuvel and TJ Osinga. The *t*-curve of multimolecular N_2-adsorption. *J. Colloid Interface Sci.* 1966; **21**, 405-14.
[50] M Nakano, H Ogawa and K Itabashi. Zeolite based adsorbents and catalysts for environmental applications utilizing a function of hydrocarbon-adsorption. *TOSOH Res. Tech. Rev.* 2001; **45**, 29-35.

[51] R López-Fonseca, BD Rivas, JI Gutiérrez-Ortiz, A Aranzabal and JR González-Velasco. Enhanced activity of zeolites by chemical dealumination for chlorinated VOC abatement. *Appl. Catal. B Environ.* 2003; **41**, 31-42.
[52] D Feller. A complete basis set estimate of cation- π bond strengths: Na^+ (ethylene) and Na^+ (benzene). *Chem. Phys. Lett.* 2000; **322**, 543-8.
[53] R Amunugama and MT Rodgers. Cation-π interactions with a model for an extended π network: Absolute binding energies of alkali metal cation-naphthalene complexes determined by threshold collision-induced dissociation and theoretical studies. *Int. J. Mass. Spectrom.* 2003; **227**, 1-20.
[54] RG Desiraju and T Stiener. *The weak hydrogen bond in the structural chemistry and biology*. Oxford University Press, Oxford, 1999.
[55] H Ito, T Iiyama, A Hamasaki, S Ozeki and S Yamazaki. Study of water adsorption on hydrophobic Na-ZSM-5 and H-ZSM-5 by directly measuring adsorption isobars and isotherms. *Chem. Lett.* 2012; **41**, 1279-81.